

A Dedicated Paediatric [18F]FDG PET/CT Dosage Regimen

Christina Cox (✉ c.cox@erasmusmc.nl)

Erasmus MC <https://orcid.org/0000-0001-5313-6727>

Daniëlle M.E. van Assema

Erasmus MC

Frederik A. Verburg

Erasmus MC

Tessa Brabander

Erasmus MC

Mark Konijnenberg

Erasmus MC

Marcel Segbers

Erasmus MC

Research Article

Keywords: Image quality, PET, [18F]FDG activity, dose optimization, patient size, body weight

Posted Date: June 2nd, 2021

DOI: <https://doi.org/10.21203/rs.3.rs-534048/v1>

License:   This work is licensed under a Creative Commons Attribution 4.0 International License.

[Read Full License](#)

Version of Record: A version of this preprint was published at EJNMMI Research on July 19th, 2021. See the published version at <https://doi.org/10.1186/s13550-021-00812-8>.

1 A dedicated paediatric [¹⁸F]FDG PET/CT dosage regimen

2

3 Christina P.W. Cox¹ Orcid ID: 0000-0001-5313-6727

4 Daniëlle M.E. van Assema¹ Orcid ID: 0000-0003-0555-7441

5 Frederik A. Verburg¹ Orcid ID: 0000-0003-1401-1993

6 Tessa Brabander ¹ Orcid ID: 0000-0002-8000-6490

7 Mark Konijnenberg ¹ Orcid ID: 0000-0001-5895-8500

8 Marcel Segbers¹

9 ¹Department of Radiology & Nuclear Medicine, Erasmus Medical Centre, Rotterdam, the Netherlands

10

11 Address:

12 Erasmus Medical Center

13 Department of Radiology & Nuclear Medicine

14 Postbus 2040 3000 CA Rotterdam

15 The Netherlands

16

17 Corresponding Author:

18

19 Christina P.W. Cox

20 Email: c.cox@erasmusmc.nl

21 Telephone number: +31107040132

22

23 Email addresses of other authors:

24 Daniëlle M.E. van Assema: d.vanassema@erasmusmc.nl

25 Frederik A. Verburg: f.verburg@erasmusmc.nl

26 Tessa Brabander: t.brabander@erasmusmc.nl

27 Mark Konijnenberg: m.konijnenberg@erasmusmc.nl

28 Marcel Segbers: m.segbers@erasmusmc.nl

29

30 **Abstract**

31

32 **Background**

33 The role of 2-[¹⁸F]fluoro-2-deoxy-D-glucose ([¹⁸F]FDG) Positron emission tomography / computed
34 tomography (PET/CT) in children is still expanding. Dedicated paediatric dosage regimens are needed to
35 keep the radiation dose as low as reasonably achievable and reduce the risk of radiation-induced
36 carcinogenesis. The aim of this study is to propose a paediatric dosage regimen based on patient size that
37 provides a constant and clinical sufficient image quality at a reasonable effective dose.

38 **Methods**

39 In this retrospective analysis 102 children (54 boys and 48 girls) were included that underwent a
40 diagnostic [¹⁸F]FDG PET/CT scan. The image quality of the PET scans was measured by the signal-to-
41 noise ratio (SNR) in the liver. The SNR liver was normalized (SNR_{norm}) for administered activity and
42 acquisition time to apply curve fitting with body weight, body length, body mass index, body
43 weight/body length and body surface area. Curve fitting was performed with two power fits, a non-linear
44 2-parameter model αp^{-d} and a linear single parameter model $\alpha p^{-0.5}$. The fit parameters of the preferred
45 model were combined with a user preferred SNR to obtain at least moderate or good image quality for the
46 dosage regimen proposal.

47 **Results**

48 Body weight demonstrated the highest coefficient of determination for the non-linear ($R^2 = 0.81$) and
49 linear ($R^2 = 0.80$) models. The non-linear model was preferred by the Akaike's corrected information
50 criterion. We decided to use a SNR of 6.5, based on the expert opinion of three nuclear medicine
51 physicians. Comparison with the quadratic adult protocol confirmed the need for different dosage
52 regimens for both patient groups. The amount of administered activity can be reduced with at least 41%

53 when compared with the current paediatric guidelines.

54 Conclusion

55 Body weight has the strongest relation with [¹⁸F]FDG PET image quality in children. The proposed non-
56 linear dosage regimen based on body mass will provide a constant and clinical sufficient image quality
57 with a significant reduction of the effective dose compared to the current guidelines. A dedicated
58 paediatric dosage regimen is necessary, as a universal dosing regimen for paediatric and adult is not
59 feasible.

60

61 **Keywords**

62

63 Image quality; PET; [¹⁸F]FDG activity; dose optimization; patient size; body weight

64

65 **Background**

66

67 Currently, the role of 2-[¹⁸F]fluoro-2-deoxy-D-glucose ([¹⁸F]FDG) Positron emission tomography /
68 computed tomography (PET/CT) imaging is still expanding in the diagnosis and follow-up of paediatric
69 oncologic, infectious and inflammatory diseases (1, 2). This expansion brings a point of concern, since
70 both the CT and the [¹⁸F]FDG expose patients to ionizing radiation, which can cause radiation-induced
71 effects later in life (3). The risk of radiation-induced carcinogenesis is higher in children, as they have a
72 longer post-radiation exposure life expectancy compared to adults (3). To reduce this risk, the radiation
73 dose of paediatric PET/CT scans should be as low as reasonably achievable (ALARA) (4) with acceptable
74 image quality and within a reasonable acquisition time. Therefore, optimization and harmonization of
75 paediatric PET/CT imaging protocols is essential(5).

76

77 For performing paediatric nuclear medicine procedures, both the Society of Nuclear Medicine and

78 Molecular Imaging (SNMMI) and European Association of Nuclear Medicine (EANM) recommend the

79 EANM paediatric dosage card (version 5.7.2016) (6, 7) or the 2016 North American Consensus
80 guidelines (NACG) (7, 8). Both these guidelines have, however, several shortcomings as they are derived
81 from adult-based protocols (9-12), and both focus on radiation dose without taking image quality into
82 account (9-13). Moreover, the EANM paediatric dosage card recommends even higher administered
83 activities per kilogram than the adult 2015 EANM [¹⁸F]FDG guidelines (14). These optimized adult
84 guidelines recommends dosage regimens based on quadratic(15) or linear relationships (16-20) between
85 administered activity, body weight and acquisition time to obtain a sufficient constant image quality.

86

87 In contrast to adult dose regimens, only a few studies have been published on optimizing administered
88 activities in children. Accorsi et al. (10) found that weight was the best patient-dependent indicator for the
89 administered activity necessary to obtain constant sufficient image quality. A pilot study of van Gent et
90 al.(21) focussed on body weight, showed that a linear relationship between body weight and administered
91 activity results in a constant image quality. Other studies have reduced the administered [¹⁸F]FDG
92 activity per kilogram of body weight based on simulations of PET low-dose scans by reduction of count
93 rates (11, 22, 23).

94

95 The Paediatric Dosage Harmonization Working Group and the 2020 paediatric guideline stated that more
96 data is needed to optimize the current guidelines (7, 24). This can be achieved by dedicated paediatric
97 studies for optimizing the [¹⁸F]FDG PET guidelines. The aim of this study, therefore, is to investigate the
98 relation between patient-dependent parameters and [¹⁸F]FDG PET image quality and to propose a
99 dedicated paediatric dose regimen that provides a constant and clinical sufficient image quality.

100

101 **Methods**

102

103 *Patients*

104 This retrospective study included 102 children (54 boys and 48 girls; mean age 12.5 ± 4.6 years; range
105 0.5-17.9 years), that underwent a diagnostic [^{18}F]FDG PET/CT scan at the Erasmus Medical Centre
106 between January 2017 and July 2020. Inclusion criteria were: preparation according to local protocol;
107 serum glucose < 7.0 mmol/L; administered activity $\pm 10\%$ of the recommended activity; PET
108 acquisition time 60 ± 5 minutes post injection and when disease was present no signs of extensive liver
109 involvement on PET images. The same criteria were used to select 85 adult patients (26 male and 59
110 female; mean age 57.0 ± 16.5 years) to compare with the paediatric results. The study was approved by
111 the Medical Ethical Committee of the Erasmus Medical Centre (MEC-2021-0078), and procedures were
112 in accordance with the Declaration of Helsinki of 1964, as revised in 2013.

113

114 *Patient-dependent parameters*

115 For each patient, the patient-dependent parameters were collected or calculated in order to investigate the
116 relationship between these parameters and [^{18}F]FDG PET image quality. Body weight (BW) [kg] and
117 body height (H) [m] were collected from the patient files. Body mass index (BMI), Body weight per body
118 height (BWH) and Body surface area (BSA) were calculated as follows:

119 Body mass index (BMI): $= \frac{M}{H^2}$ [kg/m²]

120 Body weight per body height (BWH): $= \frac{M}{H}$ [kg/m]

121 Body surface area (BSA): $= 0.007184 \times M^{0.425} \times H^{0.725}$ [m²](25)

122

123 *[^{18}F]FDG PET/CT*

124 Patients were prepared according to local protocols for [^{18}F]FDG PET/CT in children and adults. Children
125 had to fast for four hours prior to injection and were stimulated to drink water (body weight $\times 10$ ml < 10
126 years or 500-1000 ml > 10 years) during the last two hours before injection. Adults had to fast for six
127 hours and drink 1000 ml of water before injection. Additionally, 17 children and 10 adults followed a
128 carbohydrate-restricted diet for 24 hours and fasted the last 12 hours to suppress myocardial [^{18}F]FDG

129 uptake. Uptake of [¹⁸F]FDG in brown adipose tissue was suppressed in 91 children and 17 adults by
130 administering Propranolol (0.33 milligram [mg] x BW with a maximum of 20 mg one hour before the
131 injection for children and a fixed dose of 20 mg for adults. Dosing of [¹⁸F]FDG activity was determined
132 with the local linearized quadratic dose regimen of 1.7 megabecquerel per kilogram (MBq/kg) (\leq 55kg, 68
133 children, with a minimum of 14 MBq); 2.3 MBq/kg (55-70kg, 26 children); 3.0 MBq/kg (71-95 kg, 7
134 children) and 4.0 MBq/kg (\geq 96 kg, 1 child) and was intravenously injected (children median: 82 MBq;
135 range 13-392 MBq and adults median: 138MBq; range 56-532 MBq) followed by resting in a warm and
136 quiet room. PET images were acquired 60 ± 5 minutes for children and 59 ± 3 minutes for adults after
137 tracer injection in supine position on a Siemens Biograph mCT PET/CT scanner (Siemens Healthineers,
138 Erlangen, Germany). According to our local scan protocol, first a whole-body low dose CT with
139 optimized parameters (26-28) was acquired for attenuation correction and localization purposes
140 (Teenager/adult values in brackets). 80 kV (120 kV); Quality reference mAs 140 (40 mAs); Automatic
141 Exposure Control strength strong (average); rotation time 0.5 seconds; pitch 0.8 mm; slice thickness 2
142 mm (3mm); reconstructed slice thickness 2 mm (3 mm) and a Siemens B19f Low Dose for Emission
143 Computed Tomography kernel. Directly after the low dose CT, PET acquisition started with an
144 acquisition time of 3 minutes per bedposition (mbp) from the inguinal region to the skull base with the
145 arms up (61 children and all adults). Another 41 children (31 arms up, 10 arms down) were scanned from
146 the skull base to the feet with 2 mbp for the additional lower extremities. Once acquisition was finished,
147 PET scans were corrected for scatter and attenuation using the low dose CT, followed by reconstruction
148 using ordered subset expectation maximization (OSEM; 3 iterations; 21 subsets; Point Spread Function
149 (PSF) recovery; Time of Flight (TOF); a 3 mm Gaussian post reconstruction filter on a matrix of 200x200
150 with a pixel size of 4.1x4.1 mm and 3mm slice thickness.

151

152 *Image analysis*

153 The reconstructed PET scans were analyzed for image quality based on the approach as described by de
154 Groot et al. (15) and previously used by Cox et al. (29). Image quality was measured with the signal-to-

155 noise ratio (SNR) in the liver. To determine the SNR liver, a volume of interest (VOI) was placed in a
156 lesion-free homogeneous part of the right liver lobe (diameter 3 cm) using Hermes Hybrid viewer 2.6D
157 software (Hermes Medical Solutions, Stockholm, Sweden). The VOIs were placed at least 1 cm from the
158 edge of the liver to avoid partial volume effects. The SNR liver was calculated by dividing the liver
159 standard uptake value (SUV) mean normalized for body weight (SUVbw) by the standard deviation (SD)
160 (15). The liver SUV_{mean} can also be used as a measure for liver deoxyglucose metabolism (30, 31). In
161 order to compare the liver deoxyglucose metabolism between children and adults, the liver SUV_{mean}
162 normalized by body surface area (SUV_{bsa}) was determined. This value is less dependent on body size
163 and age compared to SUV_{bw} and therefore a better value for liver deoxyglucose metabolism (30, 31).

164

165 PET image quality depends on the time per bedposition and the amount of administered activity. The
166 product of these parameters is the dose time product (DTP [MBq·min]). The SNR liver can be normalized
167 (SNR_{norm liver} [(MBq·min)^{-1/2}]) for the administered activity and scan time per bedposition by assuming
168 Poisson statistics in which noise increases with the square root of the signal (15). The SNR_{norm liver} is
169 assumed independent of scan time and administered activity.

170
$$SNR_{norm\ liver} = \frac{SNR_{liver}}{\sqrt{DTP}} \quad (Eq.1)$$

171

172 *Statistical Analysis*

173 All statistical analyses were performed using Graphpad PRISM version 9. In order to test for significant
174 differences in liver deoxyglucose metabolism (liver SUV_{mean}) and image quality (SNR liver and
175 SNR_{norm liver}) between children and adults an unpaired t-test ($\alpha = 0.05$) or a Mann-Whitney U test ($\alpha =$
176 0.05) after testing the data for normality by a Shapiro-Wilk test ($\alpha = 0.05$) was performed. Furthermore, a
177 Pearson product correlation was run to determine the correlations between SNR liver and SNR_{norm liver}
178 with age in both patient groups.

179

180 The coefficient of determination (Pearson R^2) was used to select the best patient-dependent parameter
181 after curve fitting of each parameter with SNR_{norm liver}. Curve fitting was applied to the parameters by
182 using a power function (Equation 2) to obtain a non-linear dosage regimen as described before by the
183 Groot et al. (15):

$$184 \quad SNR_{norm\ liver, fit} = \alpha p^{-d}, \quad (\text{Eq.2})$$

185 where α and d are fit parameters and p is the patient-dependent parameter.

186 Curve fitting was also performed with equation 3 to obtain a linear dosage regimen:

$$187 \quad SNR_{norm\ liver, fit} = \alpha p^{-0.5}, \quad (\text{Eq. 3})$$

188 where α is the fit parameter and p is the patient-dependent parameter

189

190 Preference between the two models for each patient-dependent parameter was determined by the
191 difference between the Akaike's corrected information criterion values ($\Delta AICc$) (32).

192

193 To determine significant differences between the patient-dependent parameter fit with the highest R^2 and
194 the other patient-dependent parameters fits, the relative error between SNR_{norm liver} and SNR_{fit liver}
195 was calculated for each data point using $(SNR_{fit\ liver} - SNR_{norm\ liver})/SNR_{fit\ liver} \times 100\%$. The
196 relative error between the fits was tested with One-Way ANOVA test ($\alpha = 0.05$) or a non-parametric
197 Friedman test with additional post hoc tests after testing for normality (15).

198

199 The fit parameters of the best patient-dependent parameter were used for the dose regimen proposal. The
200 fit parameters were entered in the following expressions:

201 Combining equation 1 and 2 results in the following non-linear expression for the DTP [MBq·min] (15):

$$202 \quad DTP = \frac{SNR\ liver^2}{\alpha^2} \times p^{2d}. \quad (\text{Eq.4})$$

203 In the linear dosage regimen ($d=0.5$), DTP [MBq·min] is indicated by the following linear expression:

$$204 \quad DTP = \frac{SNR\ liver^2}{\alpha^2} \times p. \quad (\text{Eq.5})$$

205

206 Results

207

208 *Patient-dependent parameters*

209 The measurements and calculations of the paediatric patient-dependent parameters are displayed in Table

210 1.

Table 1: Paediatric patient-dependent parameters and SUV values			
<i>Parameters</i>	<i>Mean ± SD</i>	<i>Range</i>	<i>Median</i>
<i>Body weight [kg]</i>	45.9±19.9	3.8–96.0	46.5
<i>Body height [m]</i>	1.49±0.26	0.57–1.86	1.58
<i>BMI [kg/m²]</i>	19.4±4.3	11.7–33.9	18.8
<i>BWH [kg/m]</i>	29.6±9.9	6.7–55.2	29.6
<i>BSA [m²]</i>	1.5±0.5	0.3–2.5	1.7

211

212 *Liver deoxyglucose metabolism*

213 An unpaired t-test was performed to compare the liver deoxyglucose metabolism between children and

214 adults. This showed that SUV_{bsa} in children (0.57 ± 0.10) was significant lower ($t(185) = 7.82, p <$

215 0.001) compared with SUV_{bsa} in adults (0.69 ± 0.10) with a mean difference of 0.11 (95%CI, 0.09 to

216 0.14).

217

218 *Image quality*

219 To compare the SNR liver between children and adults an unpaired T-test was performed, which showed

220 a significant ($t(185) = 4.561, p < 0.001$) difference in mean SNR liver between children and adults. Also,

221 the Mann-Whitney U test to compare the SNR_{norm} liver between adults and children revealed a

222 significant ($U = 3087, p < 0.001$) difference between these two groups as displayed in figure 1. In

223 children the correlation between SNR liver and age showed a weak significant positive correlation ($r =$

224 $0.272, n = 102, p = 0.006$). For adults both SNR liver and SNR_{norm} liver showed no correlations with

225 age of respectively $r = -0.138, n = 85, p = 0.208$ and $r = -0.092, n = 85, p = 0.400$. This is in contrast to

226 SNRnorm liver in children, which strongly correlated with age in a negative direction ($r = -0.795$, $n =$
 227 102, $p < 0.001$).

228

229 **Figure 1:** Scatterplots of the SNR liver (A) and the SNRnorm liver (B) against age.

230

231 *Curve Fitting*

232 The results of the curve fitting of SNRnorm liver with patient-dependent parameters are presented in
 233 figure 2 and table 2. As can be seen body weight shows for both curves the highest R^2 (0.81 and 0.80,
 234 respectively). The non-linear model is the preferred model, according to the AICc. For this model, the
 235 Friedman test with additional Dunn-Bonferroni post hoc test revealed only a significant difference ($p <$
 236 0.05) between the fit of body weight and the fit of body height. (Table 2).

237

238 **Figure 2:** Curve fitting to determine the fit parameters for a linear and non-linear dosage regimen of the
 239 mean SNRnorm liver ($[\text{MBq} \cdot \text{min}]^{-1/2}$) versus Body weight (A), Body height (B), BMI (C), BWH (E) and
 240 BSA (E). The dashed lines represent the 95% confidence intervals of the fits.

241

Table 2: Fits of SNRnorm liver with the patient-dependent parameters.									
Patient-dependent parameters	SNRnorm liver, fit = $\alpha p^{-0.5}$			SNRnorm liver, fit = αp^{-d}					
	α	R^2	p value	α	d	R^2	p value	ΔAICc	AIC%
Body weight [kg]	2.51	0.80	-	2.23	0.46	0.81	-	1.86	23.8 vs 71.20
Body height [m]	0.51	0.47	< 0.001	0.62	1.15	0.78	0.046	88.44	<0.01 vs >99.99
BMI [kg/m²]	1.82	0.27	< 0.001	13.26	1.19	0.41	> 0.999	18.29	0.01 vs 99.99
BWH [kg/m]	2.20	0.67	< 0.001	4.73	0.74	0.78	> 0.999	33.61	<0.01 vs >99.99
BSA [m²]	0.50	0.75	0.001	0.51	0.64	0.81	0.085	23.89	<0.01 vs >99.99

242

243 We decided to use an SNR liver of 6.5 to obtain acceptable image quality after a review by three
 244 independent nuclear medicine physicians. This SNR level will reduce the risk of scans with a poor image
 245 quality, which sometimes occurred in children < 20 kg.

246 The proposed dedicated dosage regimen was obtained by combining equation 4 with an SNR liver of 6.5
247 and the fit parameters of body mass which are $\alpha = 2.23$ (95% CI 1.90 to 2.51) and $d = 0.46$ (95% CI 0.43
248 to 0.50). This resulted in the following non-linear expression for the DTP [MBq·min] with a minimum of
249 26 MBq conform the guidelines (7):

$$250 \quad DTP = 8.5 \times M^{0.92}. \quad (\text{Eq.6})$$

251

252 *Comparison of the proposed dosage regimen with the adult dosage regimen and the current paediatric*
253 *dosage regimen in guidelines.*

254 Figure 3 shows the fits of SNRnorm liver versus body weight that corresponds to the proposed non-linear
255 paediatric dosage regimen and the new Erasmus MC quadratic dosage regimen for adults. It can be seen
256 that the non-linear dosage regimen fits perfectly for children (fig. 3A) and not for adults (fig. 3B),
257 whereas a quadratic dosage regimen fits perfectly for adults and not for children. No universal dose
258 regimen could be found for children and adults together neither non-linear nor quadratic (fig. 3C).

259

260 **Figure 3:** Comparison between SNRnorm liver fits that corresponds with the proposed non-linear dosage
261 regimen (parameter d fixed to 0.46) and a quadratic dosage regimen (parameter d fixed to 1) for children
262 (A), adults (B) and both groups (C). The dashed lines represent the 95% confidence intervals of the fits.

263

264 In Figure 4, our dosage regimens with an acquisition time of 3 mbp are compared with those of the
265 EANM and NACG guidelines. As can be seen our new dosage regimen (65 MBq and 3.6 mSv (33)) will
266 reduce the amount of administered activity and radiation dose with 41 % (NACG: 111 MBq and 6.2 mSv)
267 and 63 % (EANM: 178 MBq and 9.9 mSv) for a child of 30kg, despite the higher amount of injected
268 activity compared to the dosage regimen used in the current study (51 MBq and 2.9mSv)

269

270 **Figure 4:** Comparison of [¹⁸F]FDG dosage regimens. Current study, EANM, NACG and the proposed
271 dose regimen.

272

273 **Discussion**

274

275 In this study, the relation between patient-dependent parameters and [¹⁸F]FDG PET image quality was
276 investigated in order to propose a dedicated paediatric dose regimen that aims for constant and sufficient
277 image quality. To the best of our knowledge, this study is the first that investigates the relationship
278 between paediatric patient-dependent parameters and [¹⁸F]FDG PET image quality based on SNR. This
279 study has demonstrated that body weight is the parameter with the greatest effect on [¹⁸F]FDG image
280 quality in children. Another important finding was that SNR_{norm} values were significant higher in
281 children and correlated more strongly with age than in adults. Furthermore, this is the first study
282 providing insight into the differences between paediatric and adult dosage regimens. This insight
283 emphasizes the need for a dedicated paediatric dosage regimen, especially for young children.

284

285 Liver deoxyglucose metabolism in children was shown to be significantly lower than in adults. These
286 results confirm the results obtained in a paediatric study by Yeung et al.(30). The increase in [¹⁸F]FDG
287 uptake during growth may be caused by age related changes in liver volume (34) and function of
288 hepatocytes (35, 36). Furthermore, the significant changes in body size, body composition (34, 37) and
289 blood volume during growth (37) could also account for an increase in [¹⁸F]FDG uptake. Not only body
290 size and age affected SUV measurements but also differences in uptake period, plasma glucose, recovery
291 coefficient and partial volume artefacts (38). The contribution of these factors may be limited in this study
292 due to the use of standardized protocols.

293

294 Despite lower SUV_{bsa} mean values and concomitant lower liver [¹⁸F]FDG uptake, small children showed
295 high SNR_{norm} values, which implies that less activity is needed to obtain sufficient image quality
296 (fig.1A). This is probably caused by less attenuation and scatter due to the smaller body sizes. In contrast
297 to SNR_{norm}, SNR has almost no correlation with age (fig 1B). This means that, despite the quite large

298 spread (range 4.3-8.1), the currently used dosage regimen already provides a constant image quality
299 throughout our patient population.

300

301 Body weight was the patient-dependent parameter with the highest coefficient of determination for both
302 fit models for SNRnorm. The fit parameters ($\alpha = 2.23$ and $d = 0.46$) of the preferred model are in line
303 with the fit parameters ($\alpha = 3.2$ and $d = 0.52$) obtained by van Gent et al.(21) in a paediatric pilot study of
304 20 patients. The fit of the preferred model was not significantly different from the fits of BMI, BWH and
305 BSA, even though body mass was used to define the optimal dose regimen as it is more practical than
306 BMI, BWH and BSA. Although the selected model explains 81% of variability in SNRnorm among
307 patients, the remaining 19 % was not explained. This variability might be caused by differences in patient
308 size, not covered by body weight. Unknown inhomogeneities within the liver VOIs might also cause
309 variability of SNRnorm. Nevertheless, our results are consistent with earlier adult [¹⁸F]FDG studies of de
310 Groot et al.(15) and Menezes et al.(39). These studies determined body weight with the highest
311 coefficient of determination with SNRnorm with respectively R^2 's of 0.77 (OSEM 3D + PSF + TOF) and
312 0.86 (OSEM 3D +PSF) using comparable scanners to ours. Body weight was also identified as the best
313 single predictor for image quality by Accorsi et al. (10) at a comparable R^2 of 0.86 using a different
314 camera, reconstruction method, and the noise equivalent count rate density (NECRD) as measure of
315 image quality. The NECRD is derived from the noise equivalent count rate (NECR) method (20), which
316 is considered to be more objectively related to SNR, since it is not affected by possible differences in liver
317 metabolism and reconstruction methods (40-42). Although, at that moment NECRD was not validated
318 with a visual assessment and therefore the estimated sufficient image quality and proposed dosage
319 regimen could be unreliable (43).

320

321 In contrast to the studies mentioned above, this study directly compared the models of children and adults.
322 It was not possible to find a universal dosing regimen linking paediatric and adult protocols (fig. 3). This
323 insight emphasizes the need for a dedicated paediatric dosage regimen, especially for young children.

324 These results are in agreement with the EANM adult guidelines (14), which recommends using a
325 quadratic dosage regimen, especially for patients > 75 kg, as this compensates for the lower image quality
326 caused by substantial attenuation when using a linear dosage regimen (15). In addition, they recommend
327 that the linear dosage regimen is appropriate to use for patients < 75 kg, but this is not supported by data
328 or references.

329

330 Our proposed paediatric [¹⁸F]FDG dosage regimen (acquisition time 3 mbp) showed a reduction of the
331 amount of administered activity and effective dose of 41% (NACG) and 63 % (EANM) in a child of 30
332 kg (fig. 4). Our findings broadly support the work of other studies in this area, which also found
333 reductions of 40-50% (10, 11, 22, 23), although they used other dosage regimens, scanners, and
334 reconstruction methods.

335

336 One limitation of our study is that the results are only valid for Siemens Biograph mCT scanners with an
337 OSEM 3D + PSF + TOF reconstruction. Therefore, further investigation will be necessary for other
338 systems and reconstruction methods. Another limitation is the absence of raw data due to the retrospective
339 approach. Therefore, NECR analysis of the raw data to support the SNR data was not possible. The
340 NECR data are more objective since they are not affected by differences in liver deoxyglucose
341 metabolism and reconstruction parameters. An earlier adult study of Menezes et al. (39) determined that
342 both SNR and NECR showed the best correlation with body weight. The clinical SNR analysis could be
343 replicated in a phantom study by de Groot et al. (15) and this showed that the effects of liver glucose
344 metabolism and reconstruction parameters are either rare or not as influential compared to attenuation
345 effects. Furthermore, it should be pointed out that our study has been primary concerned with optimizing
346 radiation dose from [¹⁸F]FDG rather than from both [¹⁸F]FDG and CT. The low dose CT protocols of our
347 scanners have already been optimized to reduce radiation dose (Child of 30 kg: DLP ± 75 mGy·cm and
348 1.4 mSv (44)) and to maintain sufficient image quality as with phantom studies in the past (26-28).

349

350 **Conclusion**

351

352 Body weight has the greatest effect on [¹⁸F]FDG PET image quality in children. The proposed non-linear
353 dosage regimen based on body mass will provide a constant and clinical sufficient image quality with a
354 reasonable radiation dose and present a significant reduction of the administered activity compared to the
355 current guidelines. A dedicated paediatric dosage regimen is necessary, as a universal dosing regimen for
356 paediatric and adult is not feasible.

357

358 **References**

359

- 360 1. Masselli G, De Angelis C, Sollaku S, Casciani E, Gualdi G. PET/CT in pediatric oncology. *Am J*
361 *Nucl Med Mol Imaging*. 2020;10(2).
- 362 2. Parisi MT, Otjen JP, Stanescu AL, Shulkin BL. Radionuclide Imaging of Infection and
363 Inflammation in Children: a Review. *Semin Nucl Med*. 2018;48(2).
- 364 3. Ozasa K, Shimizu Y, Suyama A, Kasagi F, Soda M, Grant EJ, et al. Studies of the mortality of
365 atomic bomb survivors, Report 14, 1950-2003: an overview of cancer and noncancer diseases. *Radiat*
366 *Res*. 2012;177(3).
- 367 4. ICRP. The 2007 Recommendations of the International Commission on Radiological Protection.
368 ICRP publication 103. *Ann ICRP*. 2007;37(2-4).
- 369 5. WHO. Communicating radiation risks in Paediatric imaging. Geneva: WHO press; 2016.
- 370 6. EANM. EANM Dosage Card (version 5.7.2016).
371 https://www.eanm.org/docs/EANM_Dosage_Card_040214.pdf. Accessed:Aug 2016.
- 372 7. Vali R, Alessio A, Balza R, Borgwardt L, Bar-Sever Z, Czachowski M, et al. SNMMI Procedure
373 Standard/EANM Practice Guideline on Pediatric (18)F-FDG PET/CT for Oncology 1.0. *Journal of*
374 *Nuclear Medicine*. 2021;62(1).
- 375 8. Treves ST, Gelfand MJ, Fahey FH, Parisi MT. 2016 Update of the North American Consensus
376 Guidelines for Pediatric Administered Radiopharmaceutical Activities. *J Nucl Med*. 2016;57(12).
- 377 9. Alessio AM, Kinahan PE, Manchanda V, Ghioni V, Aldape L, Parisi MT. Weight-based, low-
378 dose pediatric whole-body PET/CT protocols. *J Nucl Med*. 2009;50(10).
- 379 10. Accorsi R, Karp JS, Surti S. Improved dose regimen in pediatric PET. *J Nucl Med*. 2010;51(2).
- 380 11. Alessio AM, Sammer M, Phillips GS, Manchanda V, Mohr BC, Parisi MT. Evaluation of optimal
381 acquisition duration or injected activity for pediatric 18F-FDG PET/CT. *J Nucl Med*. 2011;52(7).
- 382 12. Jacobs F, Thierens H, Piepsz A, Bacher K, Van de Wiele C, Ham H, et al. Optimised tracer-
383 dependent dosage cards to obtain weight-independent effective doses. *Eur J Nucl Med Mol Imaging*.
384 2005;32(5).
- 385 13. Alkhybari EM, McEntee MF, Willowson KP, Brennan PC, Kitsos T, Kench PL. An Australian
386 local diagnostic reference level for paediatric whole-body (18)F-FDG PET/CT. *Br J Radiol*.
387 2019;92(1096).

- 388 14. Boellaard R, Delgado-Bolton R, Oyen WJ, Giammarile F, Tatsch K, Eschner W, et al. FDG
389 PET/CT: EANM procedure guidelines for tumour imaging: version 2.0. *Eur J Nucl Med Mol Imaging*.
390 2015;42(2):328-54.
- 391 15. de Groot EH, Post N, Boellaard R, Wagenaar NR, Willemsen AT, van Dalen JA. Optimized dose
392 regimen for whole-body FDG-PET imaging. *EJNMMI Res*. 2013;3(1):63.
- 393 16. Geismar JH, Stolzmann P, Sah BR, Burger IA, Seifert B, Delso G, et al. Intra-individual
394 comparison of PET/CT with different body weight-adapted FDG dosage regimens. *Acta Radiol Open*.
395 2015;4(2):1-9.
- 396 17. Halpern BS, Dahlbom M, Auerbach MA, Schiepers C, Fueger BJ, Weber WA, et al. Optimizing
397 imaging protocols for overweight and obese patients: a lutetium orthosilicate PET/CT study. *J Nucl Med*.
398 2005;46(4):603-7.
- 399 18. Halpern BS, Dahlbom M, Quon A, Schiepers C, Waldherr C, Silverman DH, et al. Impact of
400 patient weight and emission scan duration on PET/CT image quality and lesion detectability. *J Nucl Med*.
401 2004;45(5):797-801.
- 402 19. Masuda Y, Kondo C, Matsuo Y, Uetani M, Kusakabe K. Comparison of imaging protocols for
403 18F-FDG PET/CT in overweight patients: optimizing scan duration versus administered dose. *J Nucl*
404 *Med*. 2009;50(6):844-8.
- 405 20. Watson CC, Casey ME, Bendriem B, Carney JP, Townsend DW, Eberl S, et al. Optimizing
406 injected dose in clinical PET by accurately modeling the counting-rate response functions specific to
407 individual patient scans. *J Nucl Med*. 2005;46(11):1825-34.
- 408 21. van Gent M, Hamming VC, Schaar JE, Glaudemans AWJM, Willemsen ATM. Dose optimization
409 for pediatric FDG whole body PET/CT. *European Journal of Nuclear Medicine and Molecular Imaging*.
410 2019;46(11)1:S209.
- 411 22. Gatidis S, Schmidt H, la Fougere C, Nikolaou K, Schwenzer NF, Schafer JF. Defining optimal
412 tracer activities in pediatric oncologic whole-body (18)F-FDG-PET/MRI. *Eur J Nucl Med Mol Imaging*.
413 2016;43(13):2283-9.
- 414 23. Kertesz H, Beyer T, London K, Saleh H, Chung D, Rausch I, et al. Reducing Radiation Exposure
415 to Paediatric Patients Undergoing [18F]FDG-PET/CT Imaging. *Mol Imaging Biol*. 2021.
- 416 24. Lassmann M, Treves ST, Group ESPDHW. Paediatric radiopharmaceutical administration:
417 harmonization of the 2007 EANM paediatric dosage card (version 1.5.2008) and the 2010 North
418 American consensus guidelines. *Eur J Nucl Med Mol Imaging*. 2014;41(5):1036-41.
- 419 25. Du Bois D, Du Bois EF. A formula to estimate the approximate surface area if height and weight
420 be known. 1916. *Nutrition*. 1989;5(5):303-11; discussion 12-3.
- 421 26. Caan GA, Almeida AS, Segbers M. Phantom study into constant image quality of low-dose CT in
422 the pediatric population. *Eur J Nucl Med*. 2014;41(10)2:s649.
- 423 27. Caan GA, Almeida AS, Segbers M. Pediatric low-dose CT: How low can we go? *Eur J Nucl*
424 *Med*. 2016;43(11)1:s65.
- 425 28. Cox CPW, Segbers M., Straaten van M. Teenager: should one use a child or adult low dose
426 computed tomography protocol?: <https://epos.myesr.org/poster/esr/ecr2020/C-04435>. Accessed:Jul 2020.
- 427 29. Cox CPW, Segbers M, Graven LH, Brabander T, van Assema DME. Standardized image quality
428 for (68)Ga-DOTA-TATE PET/CT. *EJNMMI Res*. 2020;10:27.
- 429 30. Yeung HW, Sanches A, Squire OD, Macapinlac HA, Larson SM, Erdi YE. Standardized uptake
430 value in pediatric patients: an investigation to determine the optimum measurement parameter. *Eur J Nucl*
431 *Med Mol Imaging*. 2002;29(1):61-6.
- 432 31. Schomburg A, Bender H, Reichel C, Sommer T, Ruhlmann J, Kozak B, et al. Standardized
433 uptake values of fluorine-18 fluorodeoxyglucose: the value of different normalization procedures. *Eur J*
434 *Nucl Med*. 1996;23(5):571-4.
- 435 32. Burnham KP, Anderson, D. R. Model selection and multimodel inference: A practical
436 information-theoretic approach. 2nd ed. New York: Springer-Verlag; 2002.
- 437 33. ICRP. Radiation Dose to Patients from Radiopharmaceuticals: a Compendium of Current
438 Information Related to Frequently Used Substances. ICRP Publication 128. *Ann ICRP*. 2015;442:107-9.

- 439 34. Meier JM, Alavi A, Iruvuri S, Alzeair S, Parker R, Houseni M, et al. Assessment of age-related
440 changes in abdominal organ structure and function with computed tomography and positron emission
441 tomography. *Semin Nucl Med.* 2007;37(3):154-72.
- 442 35. Sastre J, Pallardó FV, Plá R, Pellín A, Juan G, O'Connor JE, et al. Aging of the liver: age-
443 associated mitochondrial damage in intact hepatocytes. *Hepatology.* 1996;24(5):1199-205.
- 444 36. Grasedyck K, Jahnke M, Friedrich O, Schulz D, Lindner J. Aging of liver: morphological and
445 biochemical changes. *Mech Ageing Dev.* 1980;14(3-4):435-42.
- 446 37. ICRP. Report of the task group on reference man. *Ann ICRP.* 1979;3(1-4).
- 447 38. Keyes JW, Jr. SUV: standard uptake or silly useless value? *J Nucl Med.* 1995;36(10):1836-9.
- 448 39. Menezes VO, Machado MA, Queiroz CC, Souza SO, d'Errico F, Namias M, et al. Optimization
449 of oncological (18)F-FDG PET/CT imaging based on a multiparameter analysis. *Med Phys.*
450 2016;43(2):930-8.
- 451 40. Wickham F, McMeekin H, Burniston M, McCool D, Pencharz D, Skillen A, et al. Patient-specific
452 optimisation of administered activity and acquisition times for (18)F-FDG PET imaging. *EJNMMI Res.*
453 2017;7(1):3.
- 454 41. McDermott GM, Chowdhury FU, Scarsbrook AF. Evaluation of noise equivalent count
455 parameters as indicators of adult whole-body FDG-PET image quality. *Ann Nucl Med.* 2013;27(9):855-
456 61.
- 457 42. Mizuta T, Senda M, Okamura T, Kitamura K, Inaoka Y, Takahashi M, et al. NEC density and
458 liver ROI S/N ratio for image quality control of whole-body FDG-PET scans: comparison with visual
459 assessment. *Mol Imaging Biol.* 2009;11(6):480-6.
- 460 43. Watson CC. Injected dose in pediatric PET. *J Nucl Med.* 2010;51(10):1657.
- 461 44. ICRP. Managing Patient Dose in Multi-Detector Computed Tomography (MDCT). ICRP
462 Publication 102. *Ann ICRP.* 2007;37(1):77.

463

464 **Abbreviations**

465 ¹⁸F-FDG: ¹⁸Fluorine-fluoro-2-deoxyglucose

466 PET/CT: positron emission tomography / computed tomography

467 SNR: signal-to-noise ratio

468 SNR_{norm}: normalized signal-to-noise ratio

469 ALARA: as low as reasonably achievable

470 SNMMI: Society of Nuclear Medicine and Molecular Imaging

471 EANM: European Association of Nuclear medicine

472 NACG: North American Concensus guidelines

473 BW: body weight

474 BMI: body mass index

475 BWH: body weight per body height
476 BSA: body surface area
477 MBq/kg: megabequerel per kilogram
478 OSEM: ordered subset expectation maximization
479 PSF: point spread function
480 TOF: time of flight
481 VOI: volume of interest
482 SD: standard deviation
483 DTP : dose-time-product
484 AICc: Akaike's corrected information criterion values
485 ANOVA: analysis of variance
486 NECRD: noise equivalent count rate density
487 NECR: noise equivalent count rate

488

489 **Declarations**

490

491 *Ethics approval and consent to participate*

492 The study was approved by the Medical Ethical Committee of the Erasmus Medical Centre (reference
493 number: 2021-0078).

494 *Consent for publication*

495 Not applicable

496 *Availability of data and material*

497 The data supporting our findings are available upon request.

498 *Competing interests*

499 C.P.W. Cox: not applicable

500 D.M.E. van Assema: not applicable

501 F.A. Verburg: not applicable

502 T. Brabander: not applicable

503 M. Konijnenberg: not applicable

504 M. Segbers: not applicable

505 *Funding*

506 C.P.W. Cox: not applicable

507 D.M.E van Assema: not applicable

508 F.A. Verburg: not applicable

509 T. Brabander: not applicable

510 M. Konijnenberg: not applicable

511 M. Segbers: not applicable

512 *Authors' contributions*

513 CC, DA and MC contributed to the study concepts and to the study design. CC contributed to the data

514 collection. CC, MM, MK and MS contributed to the data analyses and statistical analysis. CC, DA, FV,

515 TB, MM and MC contributed to the data interpretation, to the manuscript preparation, to the manuscript

516 editing and reviewing. All authors read and approved the final manuscript.

517 *Acknowledgements*

518 Not applicable

Figures

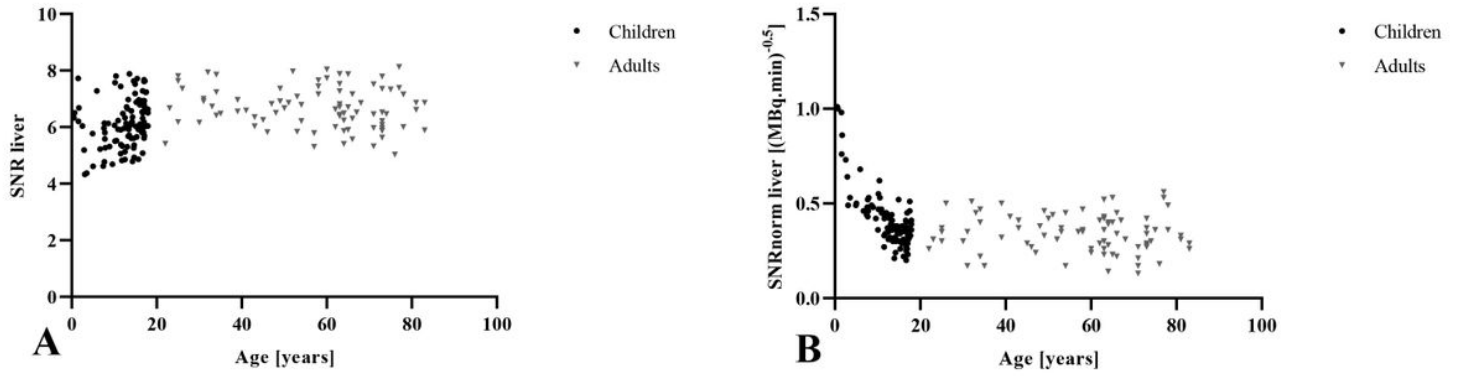


Figure 1

Scatterplots of the SNR liver (A) and the SNRnorm liver (B) against age.

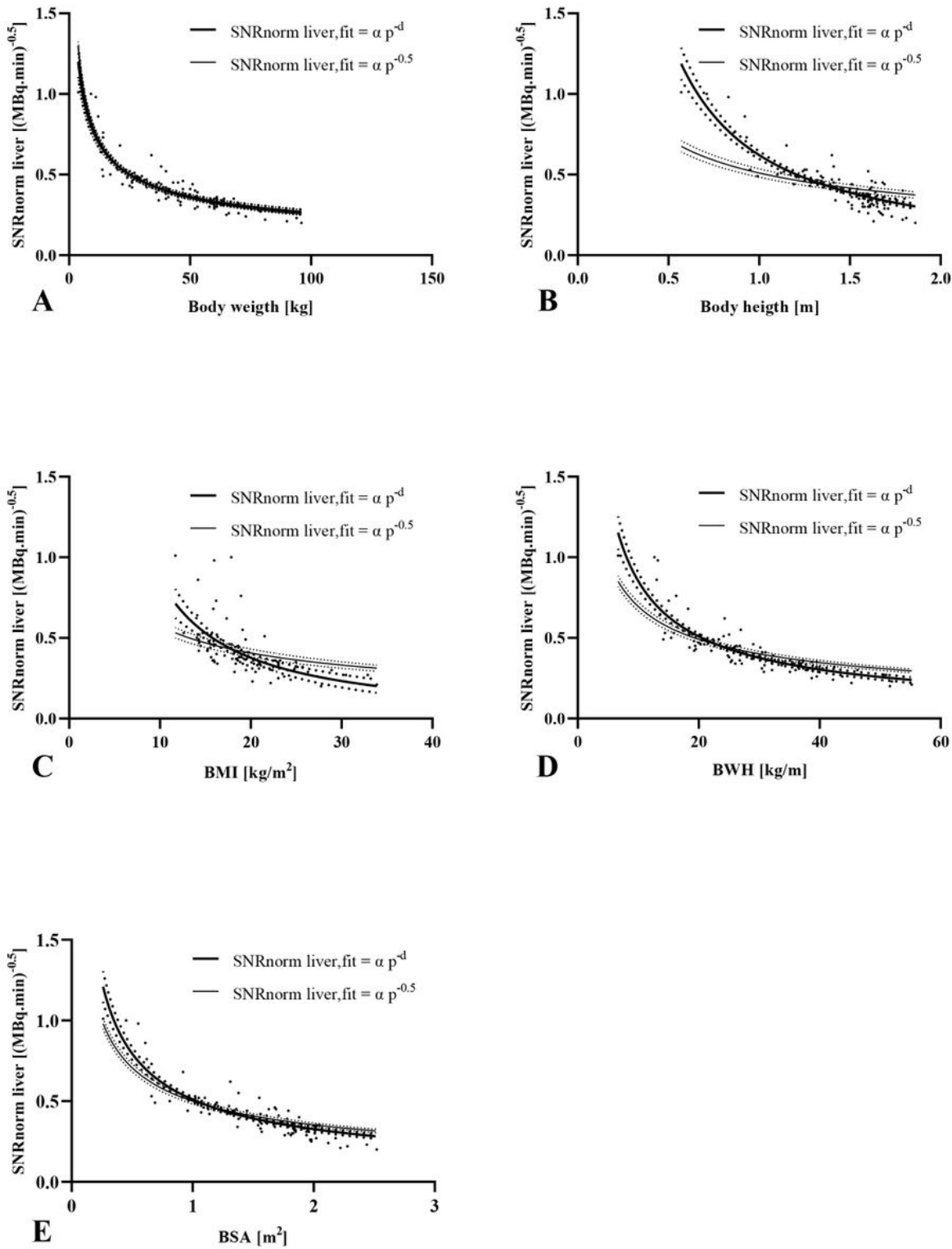


Figure 2

Curve fitting to determine the fit parameters for a linear and non-linear dosage regimen of the mean SNRnorm liver [(MBq.min)^{-1/2}] versus Body weight (A), Body height (B), BMI (C), BWH (E) and BSA (E). The dashed lines represent the 95% confidence intervals of the fits.

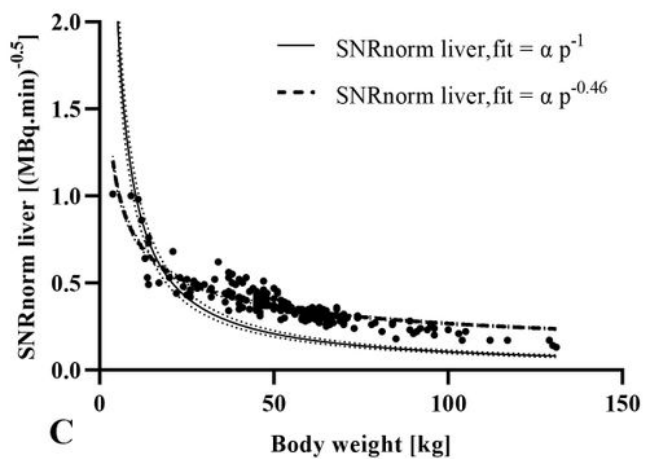
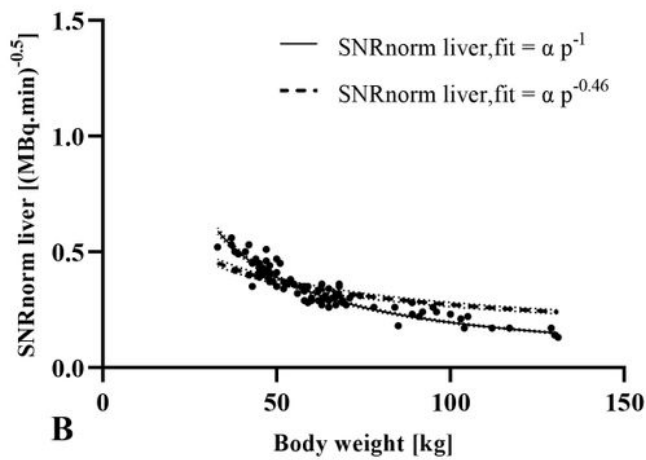
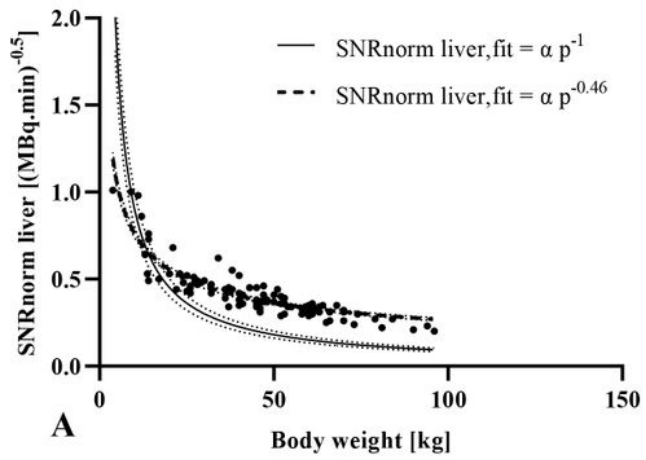


Figure 3

Comparison between SNRnorm liver fits that corresponds with the proposed non-linear dosage regimen (parameter d fixed to 0.46) and a quadratic dosage regimen (parameter d fixed to 1) for children (A), adults (B) and both groups (C). The dashed lines represent the 95% confidence intervals of the fits.

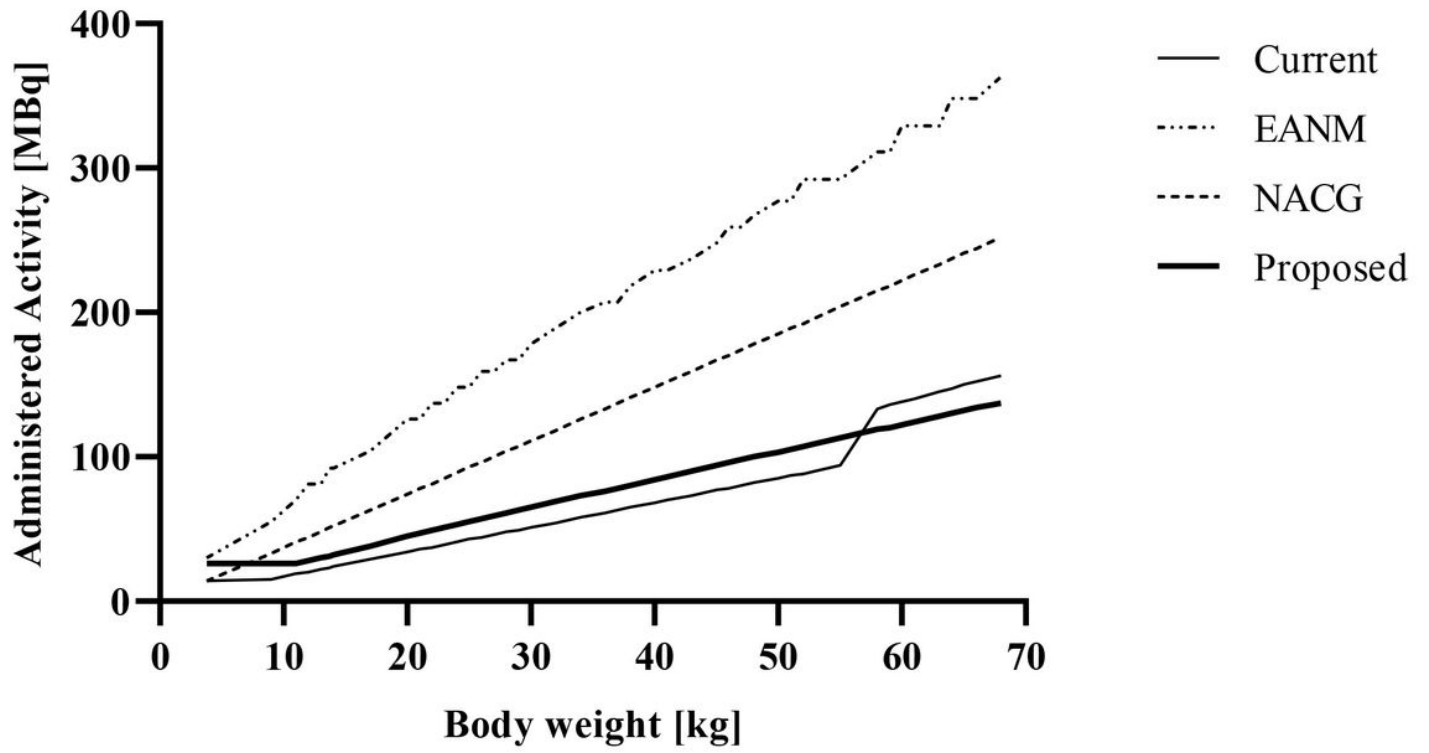


Figure 4

Comparison of [18F]FDG dosage regimens. Current study, EANM, NACG and the proposed dose regimen.